

DETERMINISTIC AND EXPERIMENTAL STUDY ON THREE-PHASE 6-PULSE RECTIFIERS

J. J. Mesas⁽¹⁾, L. Sainz⁽¹⁾ and A. Ferrer⁽²⁾

(1) Department of Electrical Engineering, ETSEIB-UPC, (2) Department of Applied Mathematics I, EPSEB-UPC
 (1) Av. Diagonal 647, 08028 Barcelona, (2) Av. Doctor Marañón, 44-50, 08028 Barcelona
 Spain

juan.jose.mesas@upc.edu, sainz@ee.upc.edu, alberto.ferrer@upc.edu

ABSTRACT

The paper introduces three-phase 6-pulse modeling with invariants. These invariants characterize rectifier behavior univocally, allowing its analysis in a simple way. Rectifier harmonic currents are also studied as a function of these invariants. Finally, the invariant model is validated and its application is described with three laboratory tests.

KEY WORDS

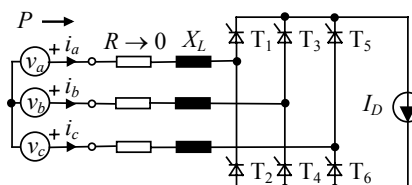
Three-phase 6-pulse rectifiers, power system harmonics, power quality

1. Introduction

There is currently great interest in harmonic load flow studies due to the increase of non-linear devices in electric power systems. Non-linear load modeling and its incorporation into load flow formulation are needed to solve the harmonic problem [1, 2]. In general, models allow the harmonic currents injected into the installations by these loads to be obtained. Apart from the magnitude, the phase angle must also be determined to completely characterize these currents.

The three-phase 6-pulse rectifier is the most widely analyzed non-linear load because it is one of the main distorting devices [3-7]. Unfortunately, analytical models are not experimentally validated or the validation is performed with few experiments. Some works are based on ratios aimed at characterizing non-linear load behavior univocally [3, 4, 5]. In [8], the rectifier behavior is univocally characterized from invariants. Invariants are the minimum number of parameters needed to completely characterize non-linear load behavior, thus these loads to be analyzed in a friendly way.

This paper presents the univocal characterization of 6-pulse controlled rectifier behavior from invariants as well as their usual range of values, which allows rectifier behavior to be studied for the rectifier usual work conditions. The harmonic currents injected by 6-pulse controlled rectifiers are analyzed from these invariants.



$$v_a(\theta) = \sqrt{2} \cdot V \cos(\theta)$$

$$v_b(\theta) = v_a(\theta - 2\pi/3), \quad v_c(\theta) = v_a(\theta + 2\pi/3)$$

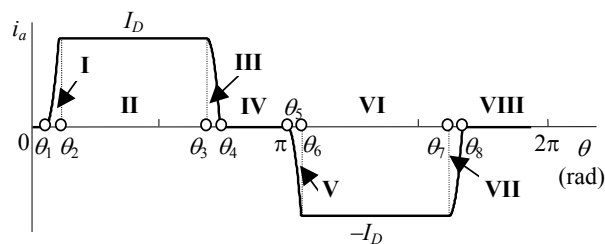


Fig. 1. Equivalent circuit and AC current waveform of the three-phase 6-pulse rectifiers.

Finally, the application and validity of the invariant model are checked with three laboratory tests.

2. Three-Phase 6-Pulse Rectifier Modelling

The equivalent circuit of the three-phase 6-pulse rectifier and its AC current i_a are shown in Fig. 1. This plot illustrates the commutation angles, which define the non-linear load current. The current characterizing the behavior of this load can be determined by analyzing the circuit topologies of the corresponding circuit, [3, 5, 8]. The considered model of the three-phase rectifier is based on the following hypotheses:

- The supply voltages are assumed to be sinusoidal and balanced, which is reasonable for voltage distortion levels and unbalance degrees in actual distribution systems, approximately 2 – 3% [3-6] and 0.5 – 1% respectively.

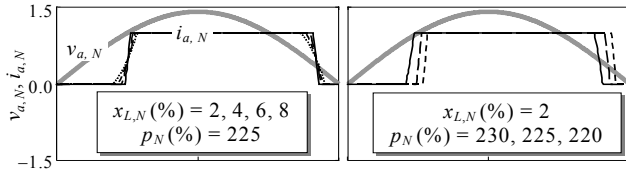


Fig. 2. Invariant influence on the 6-pulse rectifier AC current waveforms.

- The resistances of the AC supply system impedances are not considered because their influence on non-linear load behavior is much smaller than that of the inductive reactance [3-6].
- The constant current source I_D models the DC power consumption (i.e. the inductance of the DC side is considered large enough to neglect the DC current ripple) [5].

As developed in [8], the equations that characterize rectifier behavior can be normalized by using the references $U_R = V$, $I_R = I_D$ in Fig. 1, and therefore $Z_R = U_R/I_R = V/I_D$ and $S_R = U_R I_R = V \cdot I_D$. In this way, the behavior of this load, defined by the normalized variables $i_{f,N} = i_f/I_R$ ($f = a, b, c$), can be univocally characterized from the following normalized parameters:

$$x_{L,N} = \frac{X_L}{Z_R} = \frac{X_L}{V/I_D}, \quad p_N = \frac{P}{S_R} = \frac{P}{V \cdot I_D}. \quad (1)$$

These parameters are called invariants of the rectifier and their usefulness lies in the fact that they are the minimum number of parameters required to completely characterize non-linear load behavior, thus allowing its behavior to be analyzed in a friendly way.

The usual range of $x_{L,N}$ and p_N values in practical applications was obtained in [8] by relating each one of these invariants to the short-circuit ratio $R_{SC} = S_{CC}/S_{Load}$ and rectifier firing angle α , respectively. Thus, the usual values of $x_{L,N}$ and p_N are $x_{L,N}(\%) = (0.1 \dots 25)$ and $p_N(\%) = (0 \dots 233.9)$, which approximately correspond to a $R_{SC}(\text{pu}) = (5 \dots 1000)$ and a $\alpha(^{\circ}) = (0 \dots 90)$, respectively.

Finally, according to the Fourier series of the rectifier consumed currents $i_f(\theta)$ ($f = a, b, c$), the harmonic currents \underline{I}_{fh} injected by these rectifiers can be easily obtained by multiplying the normalized harmonic currents $\underline{I}_{fh,N}$ by the reference current of the load $I_R = I_D$:

$$\begin{aligned} \underline{I}_{fh} &= \frac{1}{\sqrt{2}} \frac{1}{\pi} \int_0^{2\pi} i_f(\theta) e^{-jh\theta} d\theta = \\ &= \frac{1}{\sqrt{2}} \frac{1}{\pi} \int_0^{2\pi} I_R i_{f,N}(\theta) e^{-jh\theta} d\theta = I_R \underline{I}_{fh,N} \\ &= I_D \cdot \underline{g}_{fh}(x_{L,N}, p_N) \quad (f = a, b, c ; h = 1, 5, 7, \dots) \end{aligned} \quad (2)$$

Since balanced conditions are considered, the harmonic currents are a set of positive sequence ($\underline{I}_{bh} = \underline{a}^2 \underline{I}_{ah}$ and $\underline{I}_{ch} = \underline{a} \underline{I}_{ah}$) for $h = 1, 7, \dots$ or a set of negative sequence ($\underline{I}_{bh} = \underline{a} \underline{I}_{ah}$ and $\underline{I}_{ch} = \underline{a}^2 \underline{I}_{ah}$) for $h = 5, 11, \dots$ where $\underline{a} = e^{j2\pi/3}$.

3. Three-Phase 6-Pulse Rectifier Behavior

Fig. 2 shows the influence of the invariants on the rectifier AC current waveforms. In this plot, the supply voltage waveform is also plotted. These plots were obtained from simulations performed with a MATLAB customized program considering selected $x_{L,N}$ and p_N values. It can be seen that the invariant $x_{L,N}$ mainly influences the rectifier overlap angle μ , i.e. the shape of the current waveform, (a small invariant $x_{L,N}$ leads to a small overlap angle) whereas the invariant p_N mainly influences the rectifier firing angle α , i.e. the displacement of the current waveform, (a small invariant p_N leads to a large firing angle). Considering the rectifier model used in the paper, the above rectifier behavior can be described by the relations between the firing and overlap angles, α and μ , and the proposed invariants, [5]:

$$\begin{aligned} p_N &= \frac{9}{\sqrt{6}\pi} (\cos(\alpha) + \cos(\alpha + \mu)) \\ &= \frac{3\sqrt{6}}{\pi} \cos(\alpha + \mu/2) \cos(\mu/2), \\ x_{L,N} &= \frac{\sqrt{6}}{2} (\cos(\alpha) - \cos(\alpha + \mu)) \\ &= \sqrt{6} \sin(\alpha + \mu/2) \sin(\mu/2), \end{aligned} \quad (3)$$

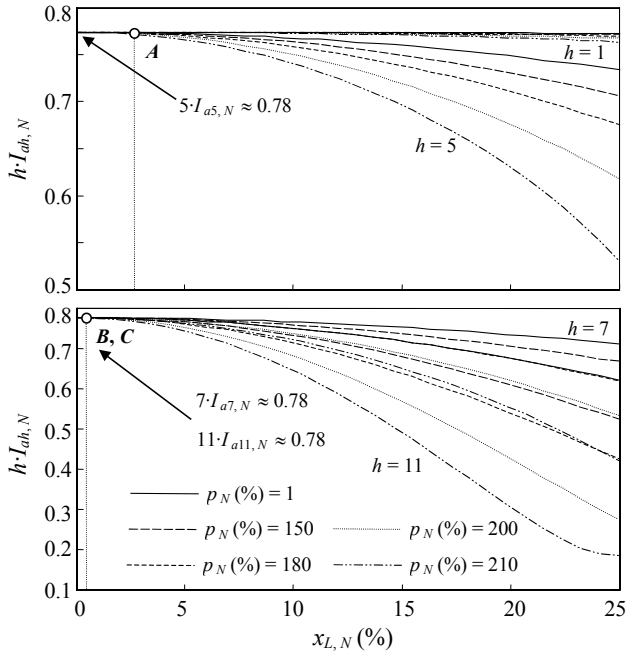
which, considering the small values of the overlap angle, can be approximated as follows:

$$\begin{aligned} p_N &\approx \frac{3\sqrt{6}}{\pi} \cos(\alpha + \mu/2) \\ x_{L,N} &\approx \sqrt{6} \sin(\alpha + \mu/2) (\mu/2) \end{aligned} \quad \Rightarrow \quad (4)$$

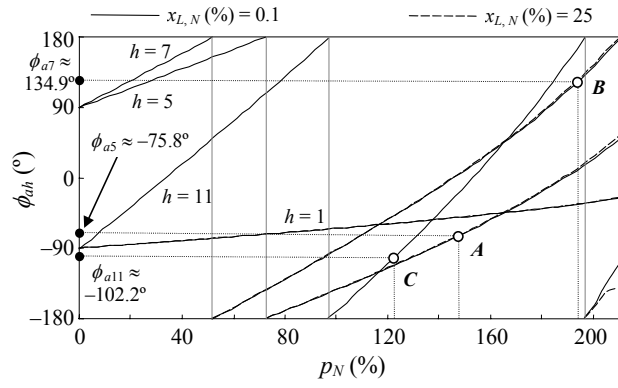
$$\alpha + \mu/2 \approx \arccos\left(\frac{p_N \pi}{3\sqrt{6}}\right), \quad \mu \approx \frac{6x_{L,N}}{\sqrt{54 - (p_N \pi)^2}}.$$

The above equations are obtained considering a good DC current smoothing. This assumption allows the rectifier behavior to be studied in a simple way, [5]. However, it is well known that the DC current ripple can be neglected only when the DC smoothing reactance is large enough.

Fig. 3 shows the harmonic spectrum (magnitude and phase angle) of the rectifier AC current of phase a . Because of the dominant influence of $x_{L,N}$ on the line current shape, Fig. 2, the fundamental and harmonic rms values are shown versus the invariant $x_{L,N}$ and for five values of the invariant p_N in Fig. 3(a). By contrast Fig. 4(b) shows the phase angles versus the invariant p_N and for two values of the invariant $x_{L,N}$ as the dominant influence of p_N on the line current displacement, Fig. 2. The current phase angles are referred to the phase angle of the supply voltage v_a . Since balanced conditions are considered, the harmonic currents of phases b and c verify



(a)



(b)

Fig. 3. Normalized fundamental and harmonic AC currents of the three-phase 6-pulse rectifier: a) Normalized rms values. b) Phase angles referred to the phase a supply voltage.

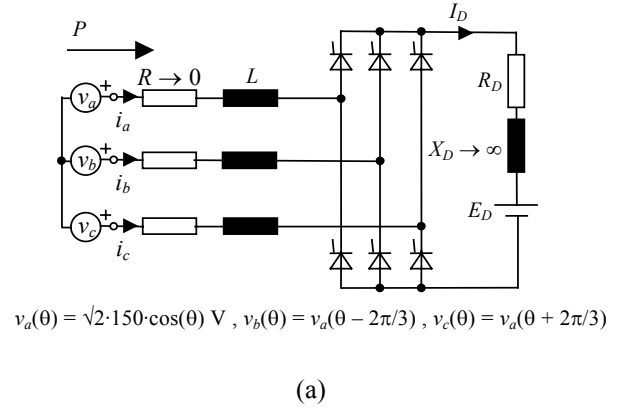
that $I_{bh,N} = \alpha^2 \cdot I_{ah,N}$ and $I_{ch,N} = \alpha \cdot I_{ah,N}$ for $h = 1, 7, \dots$, and $I_{bh,N} = \alpha \cdot I_{ah,N}$ and $I_{ch,N} = \alpha^2 \cdot I_{ah,N}$ for $h = 5, 11, \dots$ where $\alpha = e^{j2\pi/3}$. These plots were obtained from extensive simulations performed with a MATLAB customized program taking into account the usual values of the invariants.

Considering the rectifier model, the above harmonic values can be approximately described by the following formulas, [5]:

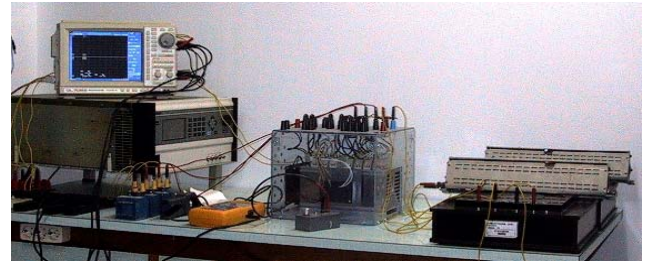
$$I_{ah,N} \approx \frac{\sqrt{6}}{\pi h} \frac{\sin(h\mu/2)}{h\mu/2}, \quad \phi_{ah} \approx \phi_{ho} - h(\alpha + \mu/2), \quad (5)$$

where $\phi_{ho} = 0$ for $h = 1, 7 \dots$ and π for $h = 5, 11 \dots$. It must be noted that

- The higher the invariant $x_{L,N}$, the higher the overlap angle μ (4), and therefore the smaller the rms value of the harmonic currents with respect to the idealized harmonic current law $(I_{h,N})_{ID} = \sqrt{6}/(\pi \cdot h)$ and according to the damping factor $[\sin(h \cdot \mu/2)]/(h \cdot \mu/2)$, (5). This attenuation is greater for high order harmonics, Fig. 3(a). The influence of the invariant p_N on the overlap angle, (4), damps the rms value of the fundamental and harmonic currents slightly.
- The smaller the invariant p_N , the higher the angle $\alpha + \mu/2$ (4), and therefore the greater the influence of this invariant on the harmonic current phase angles, (5). This influence is stronger for high order harmonics, Fig. 3(b). The invariant $x_{L,N}$ does not affect the angle $\alpha + \mu/2$ significantly, (4), and therefore does not affect the phase angle of the fundamental and harmonic currents.
- The fundamental current phase angle varies according to $\phi_{a1} \approx -(\alpha + \mu/2)$, which can be approximated to $\phi_{a1} \approx -\alpha$ for small $x_{L,N}$ values.

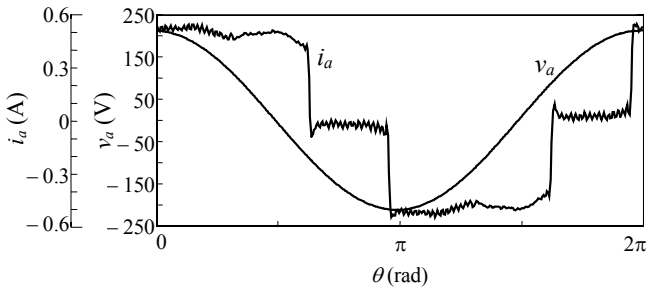


(a)



(b)

Fig. 4. Test measurements: a) Constructed circuit. b) Measuring equipment.



(a)

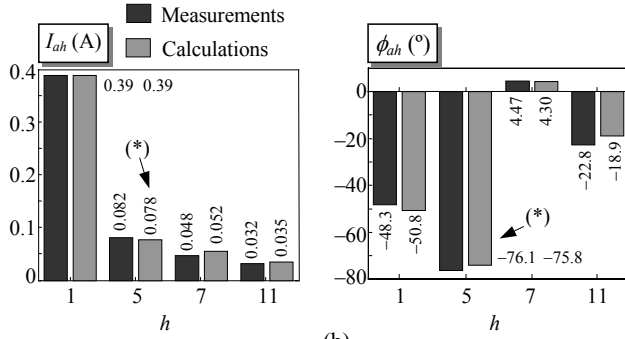
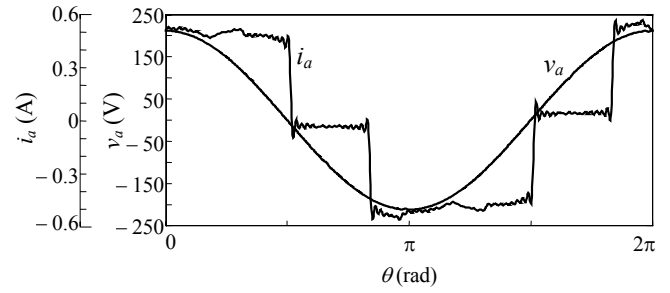
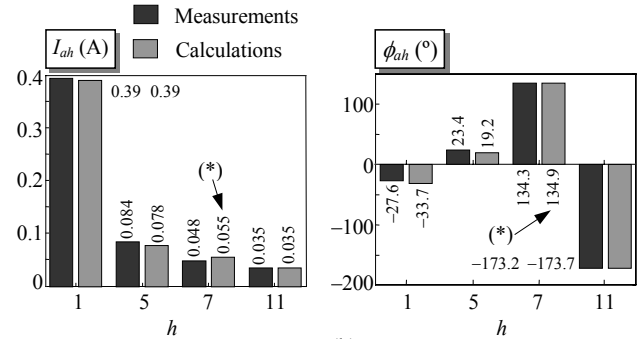


Fig. 5. Currents of the first laboratory test: a) Current waveforms. b) Fundamental and harmonic currents.



(a)



(b)

Fig. 6. Currents of the second laboratory test: a) Current waveforms. b) Fundamental and harmonic currents.

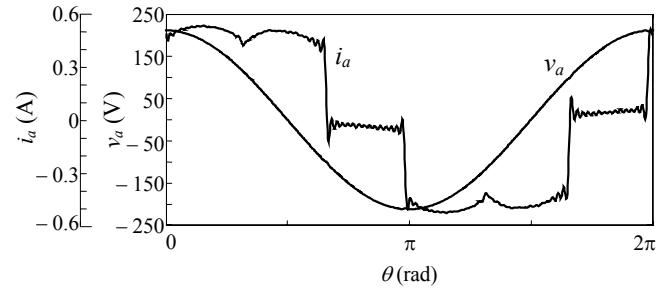
4. Experimental Study of the Three-Phase 6-Pulse Rectifier Model

Three experimental laboratory tests were performed to compare the measured currents of three-phase rectifier with the currents obtained from the invariant model. The three-phase rectifier circuit was constructed in the laboratory, Fig. 4, with three different sets of parameters,

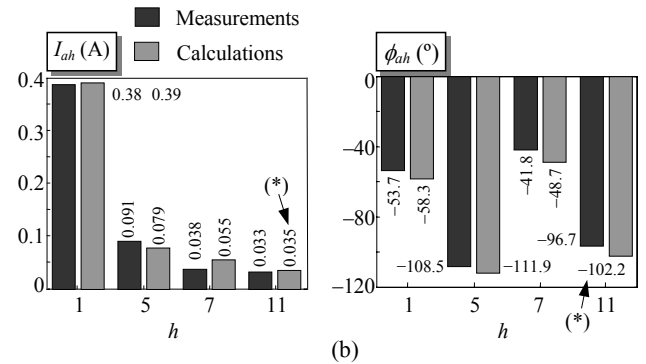
- Test #1: $L = 25.7$ mH, $I_D = 0.5$ A and $P \approx 110$ W.
- Test #2: $L = 2.45$ mH, $I_D = 0.5$ A and $P \approx 146$ W.
- Test #3: $L = 2.45$ mH, $I_D = 0.5$ A and $P \approx 92$ W.

The non-linear devices were fed by sinusoidal supply voltages of rms value $V = 150$ V generated by a power source AC ELGAR Smartwave Switching Amplifier. The voltage and current waveforms of the circuits were recorded with a YOKOGAWA DL 708 E digital scope, Fig 4(b), and treated with a computer to obtain their fundamental and harmonic components, $I_{ah} = I_{ah} \angle \phi_{ah}$, by the discrete Fourier transform. The measured current waveforms and their fundamental and harmonics are illustrated in Figs. 5, 6 and 7.

Next, the calculation with the invariant model of the fifth harmonic current corresponding to the first test (Fig. 5), the seventh harmonic current corresponding to the second test (Fig. 6) and the eleventh harmonic current corresponding to the third test (Fig. 7) is presented as an example.



(a)



(b)

Fig. 7. Currents of the third laboratory test: a) Current waveforms. b) Fundamental and harmonic currents.

$$\underline{I}_{a5} = 0.5 \cdot \underline{I}_{a5,N} \approx 0.078 \angle -75.8^\circ \text{ A.} \quad (6)$$

Test #2: As $x_{L,N} = 0.26\%$ and $p_N = 195\%$ (1), the normalized current is $\underline{I}_{a7,N} \approx 0.78/7 \angle 134.9^\circ = 0.111 \angle 134.9^\circ$ (point B in Fig. 3). Then,

$$\underline{I}_{a7} = 0.5 \cdot \underline{I}_{a7,N} \approx 0.055 \angle 134.9^\circ \text{ A.} \quad (7)$$

Test #3: As $x_{L,N} = 0.26\%$ and $p_N = 122.5\%$ (1), the normalized current is $\underline{I}_{a11,N} \approx 0.78/11 \angle -102.2^\circ = 0.0709 \angle -102.2^\circ$ (point C in Fig. 3). Then,

$$\underline{I}_{a11} = 0.5 \cdot \underline{I}_{a11,N} \approx 0.035 \angle -102.2^\circ \text{ A.} \quad (8)$$

It can be noted that the differences between the measured currents and the invariant model currents are small. The third test shows the main difference as a result of the DC current ripple.

5. Conclusion

This paper analyzes the deterministic harmonic currents consumed by three-phase 6-pulse controlled rectifiers without DC current ripple (DC smoothing reactance large enough). The study is based on the invariants of these non-linear loads, which characterize their behavior univocally and allow analyzing them in a friendly way. Several plots illustrate the invariant influence on the magnitude and phase angle of the harmonic currents. Moreover, three laboratory tests are described to show the application and validity of the invariant model.

Acknowledgement

This work was supported by grant DPI2006-2157.

References

- [1] J. Arrillaga et al., Power System Harmonics, (University of Canterbury, Christchurch New Zealand: John Wiley & Sons, 1997).
- [2] E. F. Fuchs & M. A. S. Masoum, Power quality in power systems and electrical machines, (Elsevier/Academic Press, 2008).
- [3] M. Grötzbach, M. Bauta & R. Redmann, Line side behaviour of six-pulse diode bridge rectifiers with AC-side reactance and capacitive load, *Proc. 3rd Europ. Power Quality Conf.*, Bremen, Germany, 1995, 525-534.

[4] M. Grötzbach & R. Redmann, Line current harmonics of VSI-fed adjustable-speed drives, *IEEE Trans. on Ind. Applications*, 36(2), 2000, 683-690.

[5] M. Grötzbach & R. Redmann, Analytical predetermination of complex line-current harmonics in controlled AC/DC converters, *IEEE Trans. on Ind. Applications*, 33(3), 1997, 601-612.

[6] J.G. Mayordomo et al., A contribution for modelling controlled and uncontrolled AC/DC converters in harmonic power flows, *IEEE Trans. on Power Delivery*, 13(4), 1998, 1501-1507.

[7] J.G. Mayordomo et al., Iterative harmonic analysis for controlled and uncontrolled ac/dc converters under unbalanced conditions: A compromise between model accuracy and flexibility, *Proc. 8th IEEE Int. Conf. on Harmonics and Quality of Power (ICHQP)*, Athens, 1998, 412-418.

[8] L. Sainz, J.J. Mesas, & A. Ferrer, Characterization of non-linear load behavior, *Electric Power System Research*, 78/10, 2008, pp. 1773-1783.